Kuppuswamy *et al.*
Future Journal of Pharmaceutical Sciences (2022) 8:61
https://doi.org/10.1186/s43094-022-00449-x

Future Journal of Pharmaceutical Sciences

RESEARCH

Open Access

In-silico and in-vitro analysis of novel substituted benzimidazolyl derivatives for antimycobacterial potentials targeting enoyl acyl carrier protein reductase (InhA)

Umaa Kuppuswamy[1*], Ravi Kumar Rajan[2,3], Arvinth Kumar[1] and Muthiah Ramanathan[2]

Abstract

Background: The emergence of mutated drug-resistant strains of *Mycobacterium tuberculosis* has reinvigorated the development of effective chemotherapy for MDR-TB (multidrug-resistant resistance tuberculosis). Enoyl acyl carrier protein reductase (InhA) involved in the mycobacterial fatty acid elongation system has been chosen as a potential target.

Result: All of the lead compounds had a definite Rf value and a sharp melting point, confirming that no tautomeric forms exist and that the keto (CO) group is apparent in the IR and ^{13}C NMR spectrum data. Structure-based drug design revealed the presence of amino acid residues like TYR 158, ILE 194, and PHE 149 which are crucial for InhA inhibitory activity and were considered favorable interactions. Among all, compounds 4, 5a, and 5c showed better docking and binding free energy owing to favorable interactions. Interestingly, there was a strong correlation between the binding free energy and the antimycobacterial susceptibility assay, where compounds 4, 5a, and 5c had greater activity. All the lead compounds also had good oral absorption and gut permeability. The presence of a carboxylic linker (–COOH–) between benzimidazole and the rest of the structure of the lead compounds was found to be crucial for activity as the oxygen atom and hydroxyl group of the linker formed most of the favorable interactions. The presence of chlorophenyl showed a favorable effect on InhA inhibition which might be owing to its hydrophobic interaction with PHE 149.

Conclusion: Three of the seven lead compounds synthesized had an IC value of approximately 0.5 µg/ml in the in-vitro Alamar blue assay against the *Mycobacterium tuberculosis* H37Rv strain, which is roughly comparable to the standard marketed drug, Isoniazid (INH). This manifestation of promising activity that resulted from combining in-silico and wet lab experimentation could be a great starting point for developing potent antimycobacterial agents to combat multidrug-resistant tuberculosis.

Keywords: Substituted benzimidazoles, Docking, Molecular dynamics, Synthesis, Characterization, Antimycobacterial screening, Enoyl acyl carrier protein reductase, Tuberculosis

*Correspondence: umaagangadhararao@gmail.com

[1] Department of Pharmaceutical Chemistry, PSG College of Pharmacy, The Tamil Nadu Dr. M.G.R. Medical University, Chennai, India
Full list of author information is available at the end of the article

Graphical abstract

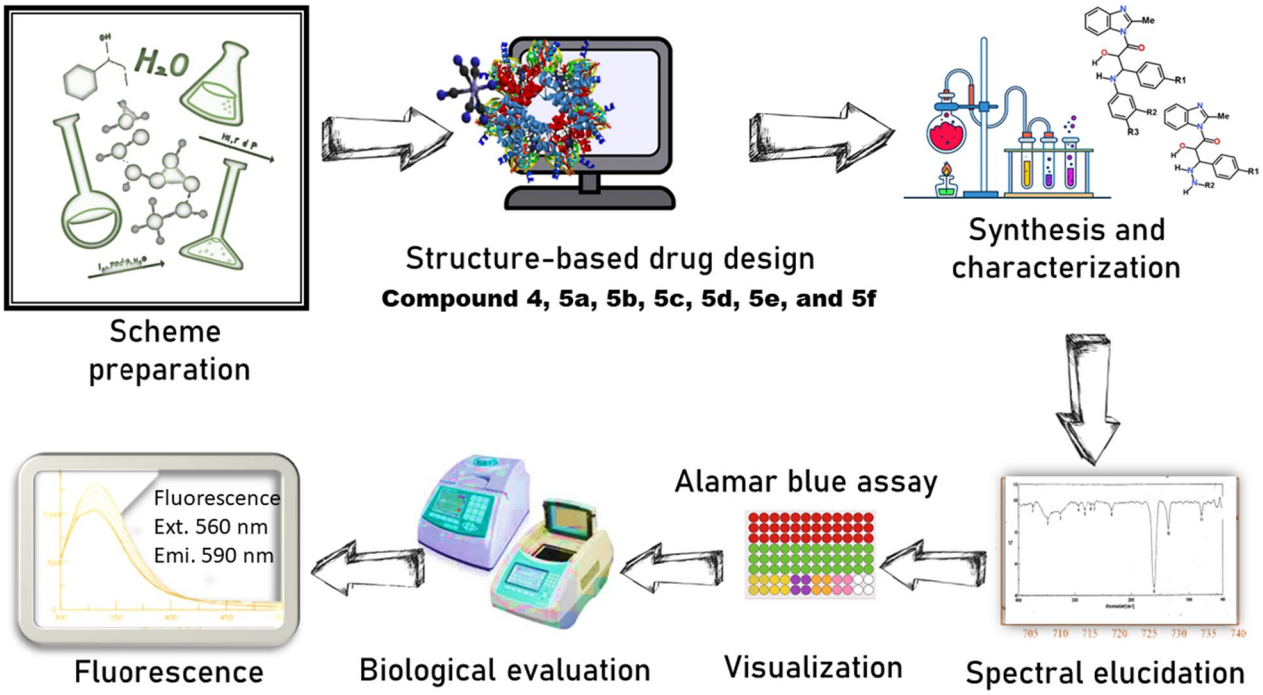

Background

Tuberculosis (TB) is a contagious disease of global influence which poses a remarkable challenge due to the evolution of resistant strains of the airborne pathogen, *Mycobacterium tuberculosis (Mtb).* In the lungs, alveolar macrophages are the first to interact with the pathogen and can befoul all the other parts of the human body later [1]. The recrudescence of the disease is inevitable due to acquired resistance. According to the WHO, around 4 lakh new MDR-TB cases are resistant to Rifampicin. Ending the TB epidemic by 2030 is predominant among the health targets of WHO [2–4]. To circumvent the problems, novel target sites and newer chemotherapeutic agents need to be identified to combat issues associated with drug resistance.

Previous studies indicated the potential pharmacophoric unit responsible for antitubercular activity such as Benzimidazole [5–7], nitroimidazopyrazinone [8], carbamates [9], triazole [10], picolinohydrazonamides [11], thiazole [12], and pyrazolopyrimidine [13]. Among these, benzimidazole derivatives have shown a variety of biological activities such as antimycobacterial, antimicrobial, antihypertensive, anticoagulant, anti-inflammatory, antifungal, and anthelmintic [14]. Even marketed drugs such as albendazole (antimicrobial), omeprazole (antiulcer), and bendamustine (anticancer) are derivatives of benzimidazole. Drugs like aminobenzimidazole-1, SB-P3G2, and SB-P8B2 (II) are extensively used in preclinical studies as an antitubercular agents [7]. The antitubercular mechanism of benzimidazole is not known so far but is expected to have three different mechanisms. Firstly, because they are structural isosteres of purines, benzimidazoles have a bactericidal effect by preventing the formation of nucleic acids and proteins. Another mechanism is the inhibition of bacterial topoisomerases by benzimidazoles. Finally, the tubulin homolog filamentous temperature-sensitive Z polymerization can also be inhibited by benzimidazole [14].

INH is reported to be involved in the mycobacterial fatty acid elongation by its interaction with Fatty acid synthetase II (FAS II). INH targets and inhibits the NADH-dependent target InhA (Enoyl acyl carrier protein reductase). Moreover, the InhA inhibitors are also reported to block the biosynthesis of mycolic acids that form the mycobacterial envelope. During our study, INH was used as a standard drug.

Due to the activation of catalase-peroxidase (Kat G), INH forms a covalent adduct with NAD co-factor. It targets the mycobacterial cell wall in a forceful manner [15]. But, the frequent occurrence of mutation in Kat G ($\geq$ 50%), inhA promoter (10–35%), and oxyR-ahpC region (10–40%) accounts for the INH resistance mechanism

which is one of the major hurdles in treating MDR-TB [16]. Hence, the direct binding of compounds with InhA that do not require activation by the mycobacterial catalase-peroxidase (Kat G) is an important strategy for treating infections caused by INH-resistant strains. Hence, enoyl acyl carrier protein reductase (InhA) was chosen as the target for initial in-silico docking studies as well as the molecular dynamics study followed by *in-vitro* screening for *Mtb*. Consequently, benzimidazolyl hydrazide derivatives have been developed which may aid to overcome the resistance associated with the Kat G mutation.

The most prevalent tool in the Pharma industry used to ponder the structure and binding free energies in a stable ligand–protein complex with high specificity is structured-based drug designing. Ranking the drug-protein complexes to identify the correct binding pose is a rational approach to drug design [17]. The MM/GBSA study provides comprehensive information on the relative binding affinities of compounds in a database. Predicting ADME by QikProp furnishes the pharmacokinetic profile of the organic molecules. Molecular dynamic studies by DESMOND help to interpret the stability of the ligand–protein complex in a biological environment. This proposed in-silico and wet lab combinational study could help in generating new leads that combat the multidrug-resistant TB.

Methods

Hardware and software

The in-silico analysis was executed in the Maestro11 modeling package provided by Schrodinger, LLC, New York, NY, 2018–4, installed in Dell precision 7820, running on Centos7OS.

Chemical scheme preparation

During the study, a scheme of about forty benzimidazolyl amino and hydrazino molecules was created. ChemSketch (version 14.01, ACD/Labsrelease2012) was used to create the 2D structures. Each structure was drawn, and its IUPAC name was identified and saved in mol format. Figure 1 depicts the steps involved in the preparation of the scheme as well as the structure of the parent molecules where the substitution has been constructed. The detailed mechanism of product formation is given in the Additional file 1.

Synthesis and characterization of the top-ranked molecule obtained after structure-based drug design

The top-ranked ligand from the structure-based drug design was taken for the synthesis. Initially, an acetylation reaction between a secondary amine and acetyl chloride produces 1-acetyl-2-methyl-1H-benzimidazole (compound 1) [18]. It is followed by the Claisen-Schmidt

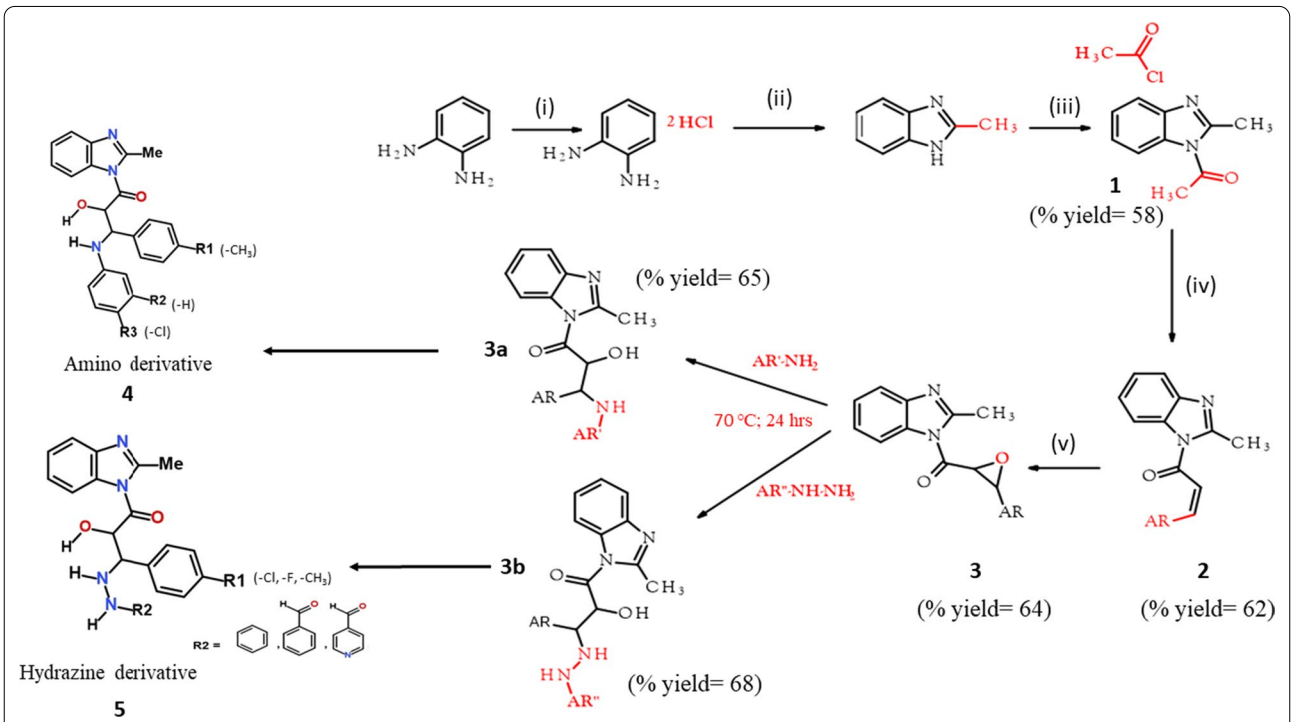

Fig. 1 Steps involved in the scheme preparation and the structure of parent molecules where the substitution was made. AR = (4-chlorophenyl, 4-flurophenyl, 4-tolyl); AR′ = (4-carboxyphenyl, 2-hydroxy, 4-carboxy phenyl), AR″ = (Nicotinoyl, phenyl, benzoyl). (i) Conc. Hcl at 100 ℃ for 30 min, (ii) 90% acetic acid at 75 ℃ for 45 min, (iii) C_2H_5OH for 3 h / add Conc. NH_3 till product precipitation, (iv) C_2H_5OH / NaOH; stirred for 4 h; left overnight, (v) Glacial CH_3COOH/H_2O_2; 3 h; kept overnight

reaction, whereby the condensation takes place at the $-COCH_3$ group due to the electronegative nature of oxygen. The condensation reaction takes place in presence of aromatic aldehydes with a dropwise addition of concentrated sulphuric acid [19]. 1-[3-(4-substituted phenyl) acryloyl]-2-methyl-1H-benzimidazole (compound 2) from 1-acetyl-2-methyl-1H-benzimidazole intermediate on treatment with hydrogen peroxide in glacial acetic acid cyclizes to an oxiranyl carbonyl derivative [20]. The basic mechanism behind cyclization is cis-hydroxylation followed by dehydration. Finally, cleavage of the epoxy ring occurs on condensation with substituted aromatic amines and hydrazides in the presence of ethanol to form 4-[1-(4-substituted phenyl)-2-hydroxy-3-(2-methyl benzimidazol-1-yl)-3-oxo-propyl] substituted aromatic amino (compound 4) and hydrazide derivatives (compound 5a-f) [20, 21]. Chemicals were procured from Hi-Media Chem Ltd., Lancaster Ltd. Macleoids Pharmaceutical Ltd., Hayman Ltd., Fischer, S.D. Fine Chem Ltd., and Loba Chemie Pvt. Ltd. The compounds obtained were purified and dried using standard methods before use. Thin-layer chromatography was carried out using silica gel G plates, and Iodine vapors were used as the visualizing agent. UV spectra were recorded on JASCOV-530 UV/VIS spectrophotometer and IR spectra were recorded on Jasco FT/IR-410 at the Department of Pharmaceutical Analysis, PSG College of Pharmacy, Coimbatore. PMR spectra were recorded at IICT, Hyderabad & IISC, Bangalore. Mass spectra were recorded at JSS College of Pharmacy, Ooty. The elemental analysis was carried out at IICT, Hyderabad.

Structure-based drug design

Molecular docking, binding free energy calculations, ADME, and a molecular dynamic study were initially performed against the InhA enzyme using different modules of Maestro v11.4 to avoid unnecessary time consumption and chemical disposal in synthesizing all of the compounds. The crystal coordinate of InhA (PDB ID: 2NSD, Resolution: 1.90Å) was taken from the RCSB PDB (protein data bank). Protein was prepared by using the Protein Preparation Wizard which utilizes OPLS3 as a forcefield for energy minimization. Post-docking minimization was performed to improve the geometry of the generated poses. The Topmost poses were selected based on the Docking and binding free energy score. The PRIME MM/GBSA (Schrödinger, LLC, and New York-4) module was used to predict the binding free energy (ΔG_{bind}) of the protein–ligand docked complexes. Several parameters related to absorption, distribution, metabolism, excretion, and toxicity are predicted by QikProp v5.4. Expensive experimental techniques, like HTS, can be avoided by accurately predicting the ADME properties beforehand to avoid testing compounds that won't work. For the molecular dynamic study, protein–ligand complexes were solvated in an orthorhombic box and entrenched in the three-site transferable intermolecular potential (TIP3P) water model. Overlapping water molecules were deleted and neutralized with Na^+ ions. The system was relaxed using the OPLS3 force field. A constant temperature at 300 K was maintained and a 2.0 fs value was obtained in the integration step. The equilibrated system was simulated for a period of 50 ns using NPT ensemble class. Finally, the root mean square deviation (RMSD) was calculated to monitor the stability of the protein [22].

Biological evaluation

Alamar blue is an oxidation–reduction dye used for antimycobacterial screening [23]. *Mtb* H_{37}Rv maintained in the Lowenstein-Jensen medium was used as the test organism [24]. All tests were carried out in duplicate. The final concentration of test compounds was such that the 200 µl of sample (100 µl of TB broth and 100 µl of bacterial suspension) contained 0.5, 1, 2.5, 5, 10, 25, 50 and 100 µg/ml of the test compound. INH was used as a standard for comparison. Well without the addition of compounds were used as blank and cells incubated with saline alone were considered as control [25]. All the cells were incubated at 37 °C. On the seventh day, 20 µl of Alamar blue solution was added to the first control well. The color changed from blue to pink, indicating sufficient growth. Therefore, the dye was added to all the wells and incubated for 6 h followed by fluorescence detection at an excitation and emission wavelength of 544 nm and 590 nm, respectively [26]. Alamar blue assay was carried out at Rajiv Gandhi Centre for Biotechnology, Trivandrum.

Statistical analysis

Data were expressed as Mean ± SD. Data analysis was done by one-way and two-way analysis of variance (ANOVA), followed by post hoc Tukey's multiple comparison test. A probability value of less than 0.001 was considered as the statistical significance criterion. All the data followed the normal distribution curve and the variance of dependent variable was same for all the data. So, the significance of the data was measured using ANOVA. GraphPad Prism 9.0 was used to do all statistical calculations (GraphPad Software, Inc. La Jolla, CA, USA).

Result

Synthesis and characterization of lead compounds obtained from structure-based drug design

Synthesis of 4-[1-(4-substituted phenyl)-2-hydroxy-3-(2-methyl benzimidazol-1-yl)-3-oxo-propyl amino] substituted aromatic amino (compound 4) and hydrazide derivatives (compound 5a–f) [19–22].

1. Synthesis of o-phenylene diamine dihydrochloride: In 1 g of Conc. Hcl, 14 g of O-Phenylene Diamine were dissolved and heated (100 °C for 30 min) with 2 g of activated charcoal. The heated filtrate was then mixed with 50 ml of conc. HCl. Filtered and immediately cooled to 10 °C in a frozen ice combination. Afterward, it is rinsed with 5 ml of conc. HCl, and was vacuum-dried using a desiccator over NaOH.

2. *Synthesis of 2-Methyl Benzimidazole:* 4.38 g of the aforementioned intermediate was heated under reflux for 45 min with 20 ml of water and 5.48 g of 90% acetic acid and heated at 75 ℃. Drops of a concentrated ammonia solution were added as the mixture cooled and the product precipitated. Then recrystallization was carried out using 10% aqueous ethanol. TLC and the solvent system (benzene/methanol – 9:1) were used to confirm purity.

3. Synthesis of intermediate 1-acetyl-2-methyl-1H-benzimidazole (compound 1): Percentage yield: 58%. 2-methyl benzimidazole (1.33 g, 0.01 mol) was dissolved in 2 ml of ethanol placed in a three-necked flask, and (0.8 ml; 0.01 mol) of acetyl chloride was added and mixed thoroughly and left for 3–4 h. A concentrated ammonia solution was gradually added, and the precipitated product was collected and crystallized from aqueous ethanol (20%) [27]. The purity of the intermediate was checked by TLC (solvent system—benzene/methanol, 9:1).

4. Preparation of 1-[3-(4-substituted phenyl) acryloyl]-2-methyl-1H-benzimidazole (compound 2) from 1-acetyl-2-methyl-1H-benzimidazole (compound 1): Percentage yield: 62%. 1-acetyl-2-methyl-1H-benzimidazole (1.76 g; 0.01 mol) was dissolved in 2 ml of ethanol placed in a three-necked flask, and sodium hydroxide solution (30 ml; 10%) was added and the mixture was cooled. To this, different substituted aromatic aldehydes (0.01 mol) dissolved in 2 ml of ethanol were added, and the mixture was stirred for 4–5 h and was left overnight [21]. Concentrated Hydrochloric acid was added drop by drop till the solution was slightly acidic. The solid separated was filtered, washed with water, and dried. The crude product was crystallized from aqueous ethanol (50%) [28], and the purity was checked by TLC [Solvent system benzene/chloroform/methanol (60:20:20)].

5. Formation of intermediate 1-{[3-(4-substituted phenyl)oxiran-2yl]carbonyl}-2-methyl-1H-benzimidazole (compound 3): Percentage yield: 64%. The 1-{[3-(4-substituted phenyl)oxiran-2yl]carbonyl}-2-methyl-1H-benzimidazole from 1 –acetyl-2-methyl-1H-benzimidazole (2.98 g; 0.01 mol) was taken in a three-necked flask and dissolved in glacial acetic acid (50 ml) and hydrogen peroxide (6 ml; 0.01 mol), and this was stirred for about 3 h and left overnight. Crushed ice was added to the reaction mixture, and the product obtained was filtered and dried. The crude product was crystallized from aqueous ethanol (50%) [20, 21]. Purity was assessed by TLC [Solvent system benzene/chloroform/methanol (60:20:20)].

6. Synthesis of the final product, 4-[1-(4-substituted phenyl)-2-hydroxy-3-(2-methyl benzimidazol-1-yl)-3-oxo-propyl amino] substituted aromatic amino and hydrazide derivatives: Percentage yield: 65% (3a) and 68% (3b). Different substituted 1-[3-(4-substituted phenyl)oxiran-2yl] carbonyl derivative compounds (3.14 g; 0.01 mol) were taken in a round-bottomed flask and ethanol (50 ml) was added. Different substituted amines or hydrazides (0.01 mol) were added and refluxed at 70 ℃ for 24 h. When the reaction ended, the volume of the reaction mixture was concentrated to half and the mixture was poured on crushed ice [20, 21]. The solid that separated was crystallized and the purity was confirmed by TLC [Solvent system benzene/chloroform/methanol (60:20:20)].

Spectral elucidation of the novel synthesized lead compounds

Compound 4

Yield: 64%, (benzene/chloroform/methanol 60:20:20), Rf = 0.580; mp 204–206 °C. λ_{max} 261 nm, IR (KBR, ν cm^{-1}): 2935 (OH), 3255 (NH), 2819 (CH), 1600 (CO), 1355 (C=C_{Ar} 771 ($CH_{Ar\ bend}$). Analytical value calculated for $C_{23}H_{20}N_3O_2Cl$ (405.00): C, 68.33; H, 4.95; N, 10.39. Found: C, 68.42; H, 4.91; N, 10.37. ^{1}H NMR (DMSO $-d_6$) δ (ppm):2.51 (3H, CH_3); 4.0–4.2 (3H, CH, OH, NH); 4.7 (1H, CH); 7.4 (Benzimidazole$_{Ar}$); 8.0 (9 H, Phenyl).^{13}C NMR (DMSO $-d_6$) δ (ppm):61 (C–Cl $_{Ar}$); 83(C); 115–140 (C_{Ar}); 201(C=O). ^{ADS}LC-MS (m/z) calculated for $C_{23}H_{20}N_3O_2Cl$: 406 [m^{+1}].

Compound 5a

Yield: 61%, (benzene/chloroform/methanol 60:20:20), Rf = 0.498; mp 203 °C. λ_{max} 278 nm, IR (KBR, ν cm^{-1}): 2988.9 (OH), 3058 (NH), 2843 (CH), 1687 (CO), 1587 (C=N), 1416 (C=C), 1178 (CN), 1093 (Cl_{Ar}), 1011 (CH_3). Analytical value calculated for $C_{23}H_{21}N_4O_2Cl$ (420.89): C, 65.57; H, 4.98; N, 13.30. Found: C, 62.48; H, 4.93; N, 13.33. ^{1}H NMR (DMSO $-d_6$) δ (ppm): 2.1 (1H, NH); 2.5 (3H, CH_3); 4.14–4.21 (2H, OH); 4.7 (2H, CH); 7.4–8.2 (13 H, aromatic). ^{13}C NMR (DMSO $-d_6$) δ (ppm):61 (C_{Clphe}); 81(C); 140 (C); 113–138 (C_{Ar}); 201 (C). ^{ADS}LC-MS (m/z) calculated for $C_{23}H_{21}N_4O_2Cl$:419.6 [m^{+1}].

Compound 5b

Yield: 62%, (benzene/chloroform/methanol 60:20:20), Rf = 0.528; mp 175–177 °C. λ_{max} 279 nm, IR (KBR, ν cm^{-1}): 3453 (NH), 2729 (OH), 2811 (CH), 2350 (CO), 1594 (C=N), 1351 (C=C), 1089 (Cl_{Ar}), 1002 (CH_3). Analytical value calculated for $\mathbf{C_{24}H_{21}N_4O_3Cl}$ (448.90): C, 64.15; H, 4.67; N, 12.47. Found: C, 64.21; H, 4.72; N,

12.43. ^{1}H NMR (DMSO $-d_6$) δ (ppm): 2.0 (1H, NH); 2.51 (3H, CH_3); 4.1–4.2 (2H, CH, OH); 4.7 (1H, CH); 7.6 (5 H, Ar), 8.1 (5H, Ph Ar). ^{13}C NMR (DMSO $-d_6$) δ (ppm):60 (C_{ClPhen}); 80 (C, C=O, CH); 141 (C, C=N); 115–140 (C_{Ar}); 168 (C, CONH); 201 (C, C=O). LC–MS (m/z) calculated for **$C_{24}H_{21}N_4O_3Cl$: 448.90** $[M+H]_+$. Found: 449.6$[M-H]_+$.

Compound 5c

Yield: 64%, (benzene/chloroform/methanol 60:20:20), Rf = 0.462; mp 168–170 °C. IR (KBR, ν cm^{-1}): 2992.98 (OH), 3054 (NH), 2839 (CH), 1684 (CO), 1592 (C=N), 1425 (C=C), 1176 (CN), 1093 (Cl $_{Ar}$), 1019 (CH_3). Analytical value calculated for $C_{23}H_{20}N_5O_3$ Cl (449.5): C, 61.46; H, 4.45; N, 15.59. Found: C, 61.57; H, 4.40; N, 15.62. ^{1}H NMR (DMSO $-d_6$) δ (ppm): 2.0 (1H, NH); 2.5 (3H, CH_3); 4.0–4.3 (3H, CH, OH, NH); 7.3–7.5 (4 H, Ar); 8.0–8.2 (9H, Ar). ^{13}C NMR (DMSO $-d_6$) δ (ppm):60 (C, CH); 80(C, C=O, CH); 115–140 (CAr); 150 (C pyridyl); 167 (C, CONH); 200 (C, CO). LC–MS (m/z) calculated for $C_{23}H_{20}N_5O_3$ Cl: 449.5$[M+H]_+$. Found: 448.1$[M-H]_+$.

Compound 5d

Yield: 60%, (benzene/chloroform/methanol 60:20:20), Rf = 0.523; mp 176 °C. λ_{max} 280 nm, IR (KBR, ν cm^{-1}): 3444 (NH), 2811 (OH), 1685 (CO), 1594 (C=N), 1351 (C=C), 119.5 ($F_{Ar\ bend}$). ^{1}H NMR (DMSO $-d_6$) δ (ppm):2.0 (1H, NH); 2.5 (3H, CH_3); 5.5 (1H, 4.0–4.3 (3H, NH, OH, CH); 6.8–7.8 (13 H, Ar). ^{13}C NMR (DMSO $-d_6$) δ (ppm): 83 (C); 140 (C); 114–139 (C_{Ar}); 16 (C, CONH); 201 (C). LC–MS (m/z) calculated for **$C_{24}H_{21}N_4O_3F$:** (432): $[M+H]_+$. Found: 431$[M-H]_+$.

Compound 5e

Yield: 58%, (benzene/chloroform/methanol 60:20:20), Rf = 0.568; mp 173–175 °C. λ_{max} 274 nm, IR (KBR, ν cm^{-1}): 3089 (NH), 2935 (OH), 2859.9 (CH), 2679 (CO), 1587 (C=N), 1342 (C=C), 1009 (CH_3). ^{1}H NMR (DMSO $-d_6$) δ (ppm):2.51 (3H, CH_3); 2.0 (1H, NH); 4.14–4.21 (2H, OH, CH); 8.1 (1H, NH); 7.2–7.6 (8 H, Ar).^{13}C NMR (DMSO $-d_6$) δ (ppm): 63 (C), 80 (C); 115–140 (C_{Ar}); 168 (C_{Ph}); 201 (C).

Compound 5f

Yield: 55%, (benzene/chloroform/methanol 60:20:20), Rf = 0.535; mp 174–176 °C. λ_{max} 280 nm, IR (KBR, ν cm^{-1}): 3482 (NH), 2929 (OH), 2811 (CH), 1594 (C=N), 1351 (C=C), 1039 (CH_3). ^{1}H NMR (DMSO $-d_6$) δ (ppm): 2.51 (3H, CH_3); 4.0–4.2 (3H, CH, OH, NH); 4.7 (1H, OH); 7.4–8.0 (13 H, aromatic). ^{13}C NMR (DMSO $-d_6$) δ (ppm):61 (C); 83 (C); 115–140 (C_{Ar}); 120–130 (C_{Ph}); 201 (C).

Table 1 Docking score and MM/GBSA ΔG_{bind} score of lead benzimidazolyl amino derivatives

Compound	R_1	R_2	R_3	Docking score (kcal/mol)	MM/GBSA score (kcal/mol)
4	0	–H	–Cl	− 11.375	− 73.97

Table 2 Docking score and MM/GBSA dG bind score of lead benzimidazolyl hydrazide derivatives

Compound	R_1	R_2	Docking score (kcal/mol)	MM/GBSA ΔG_{bind} Score (kcal/mol)
5a	–Cl	C_6H_5–	− 11.161	− 71.81
5b	–Cl	C_6H_5CO–	− 12.089	− 68.95
5c	–Cl	C_6H_4NO–	− 12.778	− 70.39
5d	–F	C_6H_5CO–	− 11.836	− 65.05
5e	0	C_6H_5–	− 11.2	− 70.32
5f	0	C_6H_5CO–	− 12.303	− 65.91
INH	–	–	− 10.283	− 67.39

Molecular interaction of lead compounds with InhA

All molecules were docked against enoyl acyl carrier protein reductase (PDB ID: 2NSD). The docking score and binding free energy of all the benzimidazolyl amino and benzimidazolyl hydrazide derivatives are given in Tables 1 and 2, respectively. The top posed structure from the docking study was taken as lead compound (4, 5a, 5b, 5c, 5d, 5e & 5f) based on the docking and MM/GBSA binding free energy score. Among the lead compounds, Compound 4 was a benzimidazolyl amino derivative and the rest were benzimidazolyl hydrazides derivatives (5a-f). The molecular interaction between different amino acids and lead compounds along with INH is demonstrated in Fig. 2. The molecular interactions observed with each molecule are discussed below.

Compound 4 formed two hydrogen bond interactions and one Π-Π stacking. One hydrogen bond donor interaction was formed between ILE 194 and the hydroxyl group of the carboxylic linker and one hydrogen bond acceptor interaction was formed between LYS 165 and 3-amino of benzimidazole pharmacophore. A pi-pi stacking was made between chlorophenyl and PHE 149. All other lead compounds made a similar hydrogen bond interaction between the linker hydroxyl group and ILE 194 was observed. In compound 5e, the linker hydroxyl group made two hydrogen bond acceptor–donor interactions with ILE 194. Other than ILE 194, compounds 5b & 5f showed a hydrogen bond acceptor interaction between the oxygen atom of the terminal benzamide group and TYR 158. In the case of INH, hydrogen bond acceptor

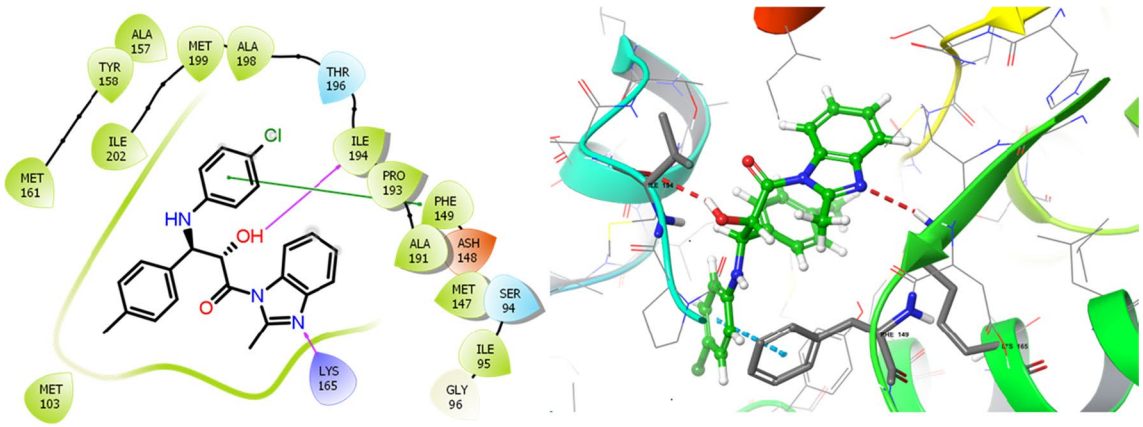

Compound 4

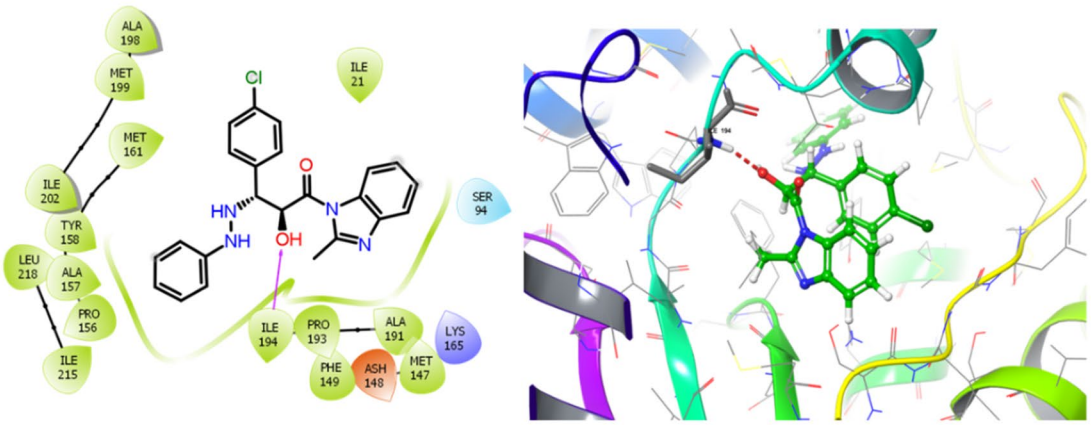

Compound 5a

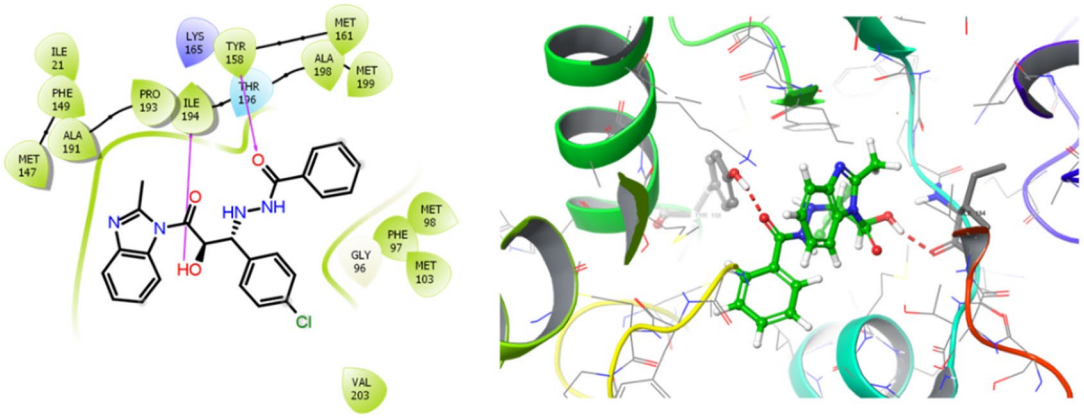

Compound 5b

Fig. 2 Interaction of InhA with the seven best lead compounds generated using 2D-lignad interaction diagram of GLIDE module

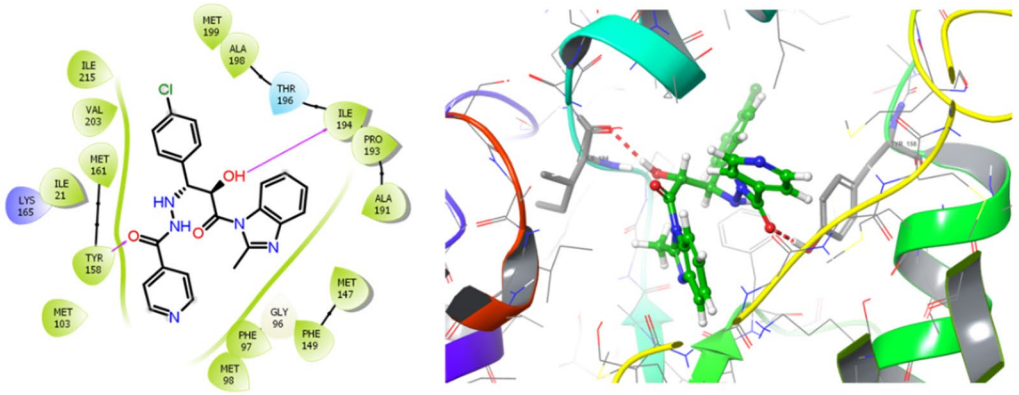

Compound 5c

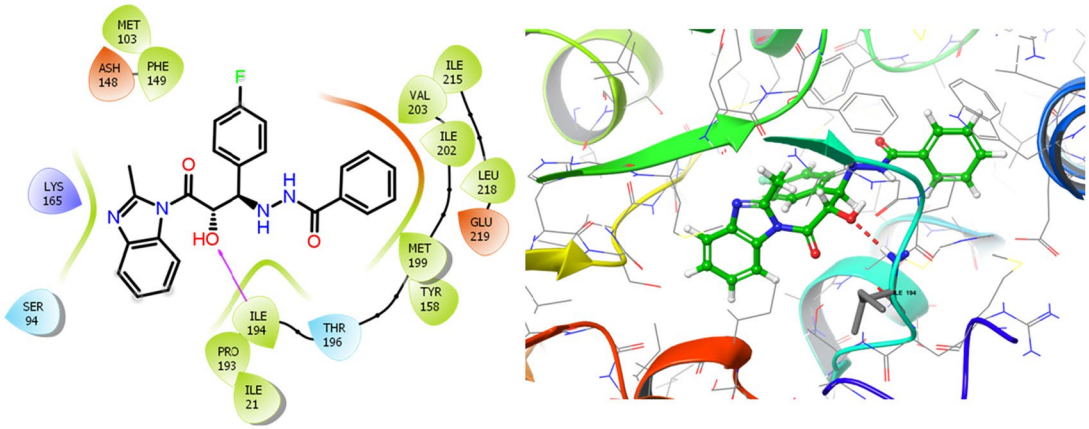

Compound 5d

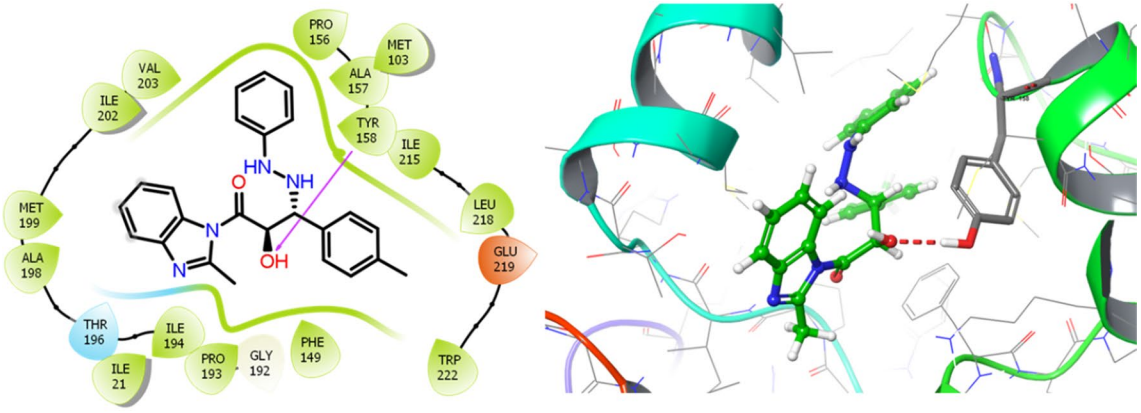

Compound 5e

Fig. 2 continued

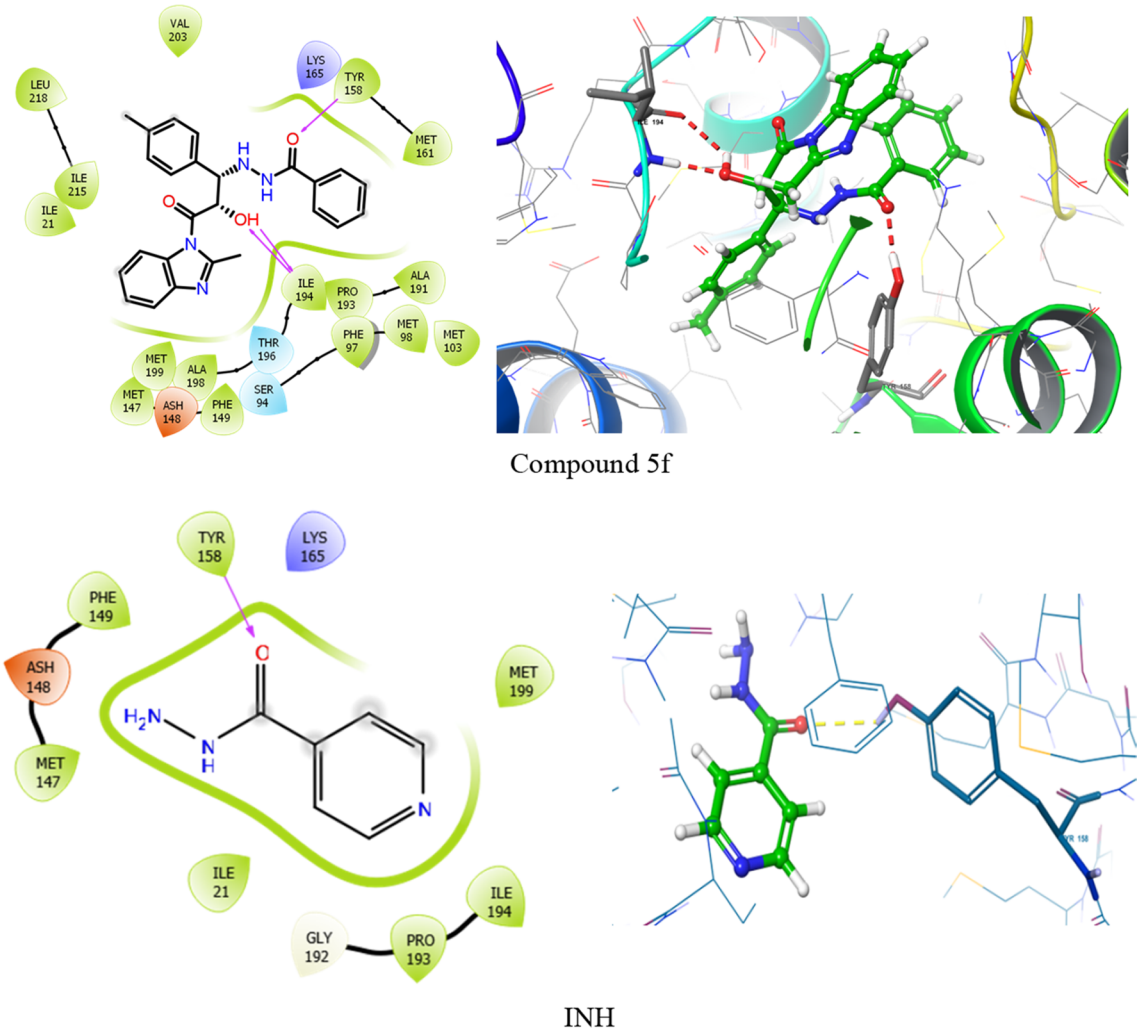

Fig. 2 continued

interaction was made between the oxygen atom of pyridine-4-carboxamide. During the study, all the lead compounds and INH showed similar amino acid interactions which were previously described as crucial for antitubercular activity (Table 3).

ADME/tox prediction of lead compounds

ADME prediction was done for the parameters such as Lipinski's rule of five, Jorgensen's rule of three, CNS activity, HERG K+ channel toxicity, Pcaco (nm/s), logBB, PMDCK (nm/s) & % Human oral absorption. Zero violation in RO5 and RO3 indicates that the molecules have a drug-like characteristic and can be orally available. The selected molecules showed lower CNS activity and lower permeability to the blood–brain barrier, which implies fewer CNS side effects. Permeability to the gut-blood barrier indicated by Pcaco was found to be excellent.

Table 3 Docking interactions of selected lead compounds

Compound	H-Bond	Pi-Pi stacking
4	ILE 194, LYS 165	PHE 149
5a	ILE 194	NIL
5b	ILE 194, TYR 158	NIL
5c	ILE 194, TYR 158	NIL
5d	LYS 165	NIL
5e	TYR 158	NIL
5f	ILE 194, TYR 158	NIL
INH	TYR 158	NIL

According to previous literature four amino acid interactions namely TYR 158, ILE 194, PHE 149 and LYS 165 are crucial for InhA inhibitory activity [29–31]

The percentage of human oral absorption emphasizes an excellent oral absorption of the novel compounds, which also corresponds to good oral bioavailability (Table 4).

Molecular dynamics study of lead compounds

A molecular dynamics study suggests that although not much conformational change was observed in the protein but for test molecules, conformational changes were more significant inside the binding pocket except for compound 5b. RMSD for all lead compounds was found to be stable at least after 35 ns was seen below 3 Å, which implies that the compounds formed a stable complex with InhA (Fig. 3). Interaction fraction analysis (molecular dynamics) showed that the majority of interaction was hydrophobic (Fig. 4). The majority of H-bond interaction that the lead compounds made was with TYR 158, ILE 194, and THR 196 (Fig. 5).

Biological screening

Antibacterial screening

The seven newly synthesized HIT compounds were screened for antibacterial activity against gram-positive *Staphylococcus aureus* and gram-negative *Escherichia coli* at a concentration of 250 µg/disk and 500 µg/disk. The results were compared with the standard drug Ciprofloxacin at 10 µg/ disk using DMSO as the vehicle [32, 33]. Novel compounds were inactive against gram-positive *Staphylococcus aureus*. Compounds 5a, 5b, and 5c exhibited mild activity at 500 µg/disk concentration, and 4, 5d, 5e, and 5f, showed moderate activity against Gram-negative *Escherichia coli*, at both 500 µg/disk and 250 µg/disk concentration.

Antimycobacterial susceptibility test using Alamar blue

The seven HIT molecules were evaluated for their antimycobacterial potentials using the Alamar blue assay model. Among the compounds screened for antitubercular activity using INH as standard, the compounds 5d & 5f showed an inhibitory concentration (IC_{50}) of 5.38 and 5.13 µg/ml respectively. The compounds 5b & 5e had IC_{50} values of 1.02 and 0.95 µg/ml respectively. The compounds 4, 5a & 5c exhibited a highly significant inhibitory concentration of 0.51, 0.56 and 0.57 µg/ml which is equipotent to the standard marketed drug INH (IC_{50} = 0.52 µg/ml). A dose-dependent percentage reduction in Alamar blue (resazurin to resorufin) by all the test compounds was observed. With an increased dose, the percentage reduction of resazurin also declined. The amount of percentage reduction is directly proportional to the lower metabolically active cells and vice versa. There was no significant difference found when INH was compared to test compounds. There were high levels of percentage reduction in Alamar blue were observed in the control group when compared to INH and test compounds. Among all, compounds 4, 5a, and 5c treated well showed significant reduction ($P < 0.001$) in percentage reduction of Alamar blue by mycobacterium when compared to control. This shows significant inhibition of mycobacterium cell by compounds 4, 5a, and 5c. All the comparative data are given in Fig. 6.

Discussion

The basic moiety, 2-methyl benzimidazole, has been reported to possess antitubercular activity [34, 35]. Benzimidazole moiety has been often used as a part of mycobacterial gyrase inhibitors as well as MtbFtsZ inhibitors, named after "filamenting temperature-sensitive mutant Z" [36]. This is the first protein to move to the division site during cell division and is essential for recruiting other proteins that produce a new cell wall between the dividing cells [37]. Considering the importance of benzimidazole moiety as an antimycobacterial principal segment, we have chosen the compounds with functionalized benzimidazole for the present in-silico and in-vitro analysis. Enoyl-acyl carrier protein reductase (InhA) is a prominent target of the current first-line drug INH, used in the treatment of tuberculosis infections [38, 39]. All our lead compounds showed a specific Rf value and a sharp melting point and therefore we confirm that there are no tautomeric forms present and the keto (CO) group appears to be visible in the IR and ^{13}C NMR spectrum data.

In-silico analysis by docking, MM/GBSA ΔG_{bind}, MD simulation, and ADME prediction resulted in bringing

Table 4 Preliminary QikProp ADME predicted data for the seven best lead molecules

Compound	CNS	log HERG	Pcaco (nm/s)	logBB	PMDCK (nm/s)	% HOA	Ro5	Ro3
4	0	− 5.619	1357.62	− 0.46	1696.26	100	0	0
5a	1	− 8.035	503.807	− 0.06	542.518	100	0	0
5b	− 1	− 6.746	682.273	− 0.92	806.375	100	0	0
5c	− 2	− 5.28	508.94	− 1.04	326.529	87.52	0	0
5d	− 1	− 6.768	679.022	− 0.98	587.325	100	0	0
5e	1	− 8.02	504.055	− 0.24	261.002	100	0	0
5f	− 2	− 6.863	580.952	− 1.19	275.051	100	0	0

*HOA (Human oral absorption), Ro5 (Rule of five), Ro3 (Rule of three)

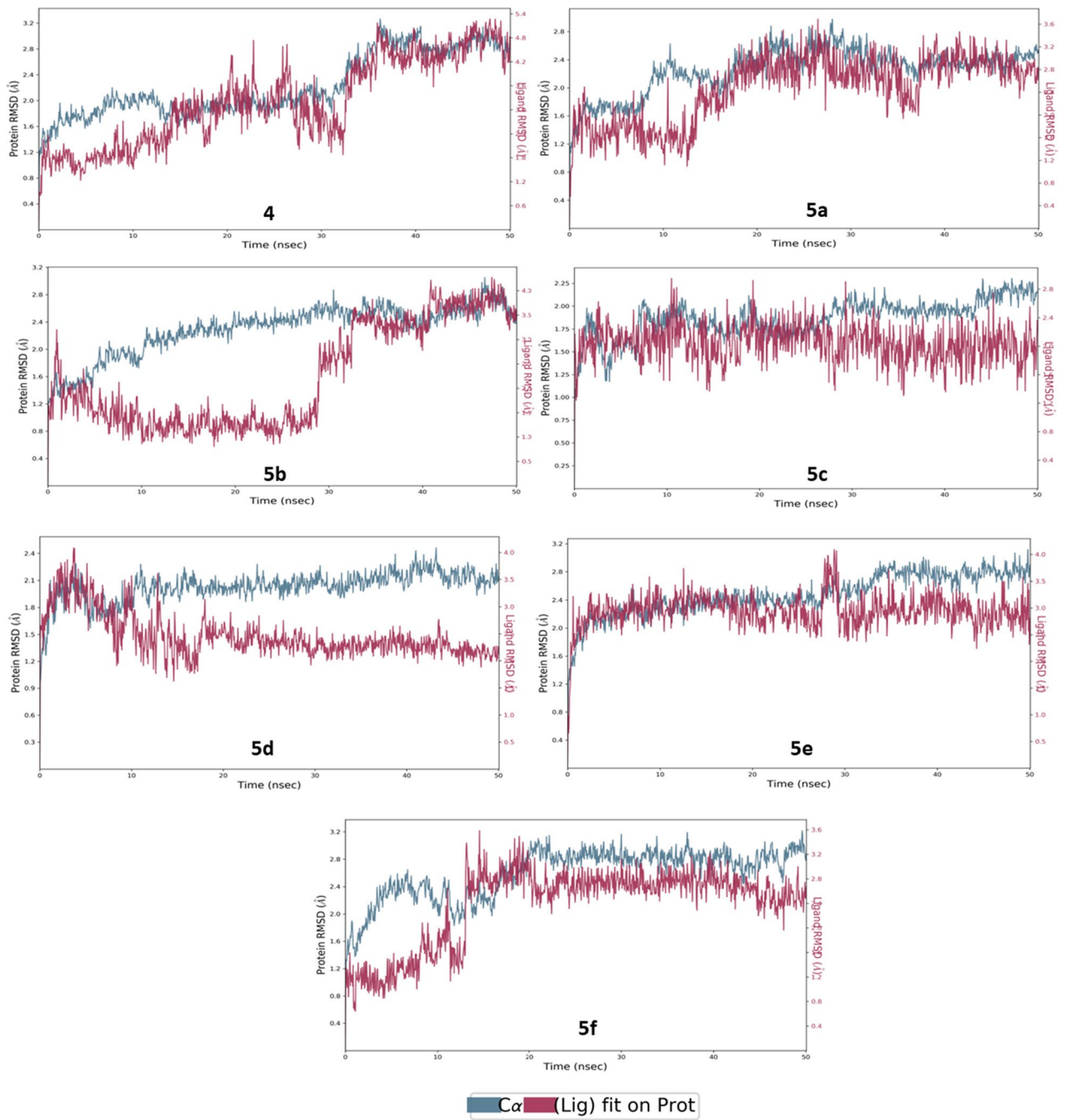

Fig. 3 Protein–Ligand RMSD of lead compounds. Compound 4 = 3.2 & 5.2 Å, Compound 5a = 2.4 & 3.63 Å, Compound 5b = 3.2 & 4 Å; Compound 5c = 2.25 & 2.8 Å; Compound 5d = 2.4 & 4 Å; Compound 5e = 3.2 & 4 Å; Compound 5f = 3.2 & 3.6 Å

out novel seven HIT compounds having a good binding profile with the target, InhA. According to the ADME prediction by QIKPROP, the parameters selected were CNS, log HERG, PCaco (nm/s), logBB, PMDCK (nm/s), % Human oral absorption, Rule of five, and Rule of three. All the three compounds bear PCaco-2 values greater than 500 nm/sec which denotes good cell permeability. The blood–brain partition coefficient for oral drugs and the predicted CNS activity does not fall within the specified range and the above drugs are expected, not to enter the BBB. Hence the untoward CNS effects could be prevented. The HIT compounds satisfy Lipinski's Rule of Five and Jorgensen's rule of three without any violations. This is also an added fact that the compounds

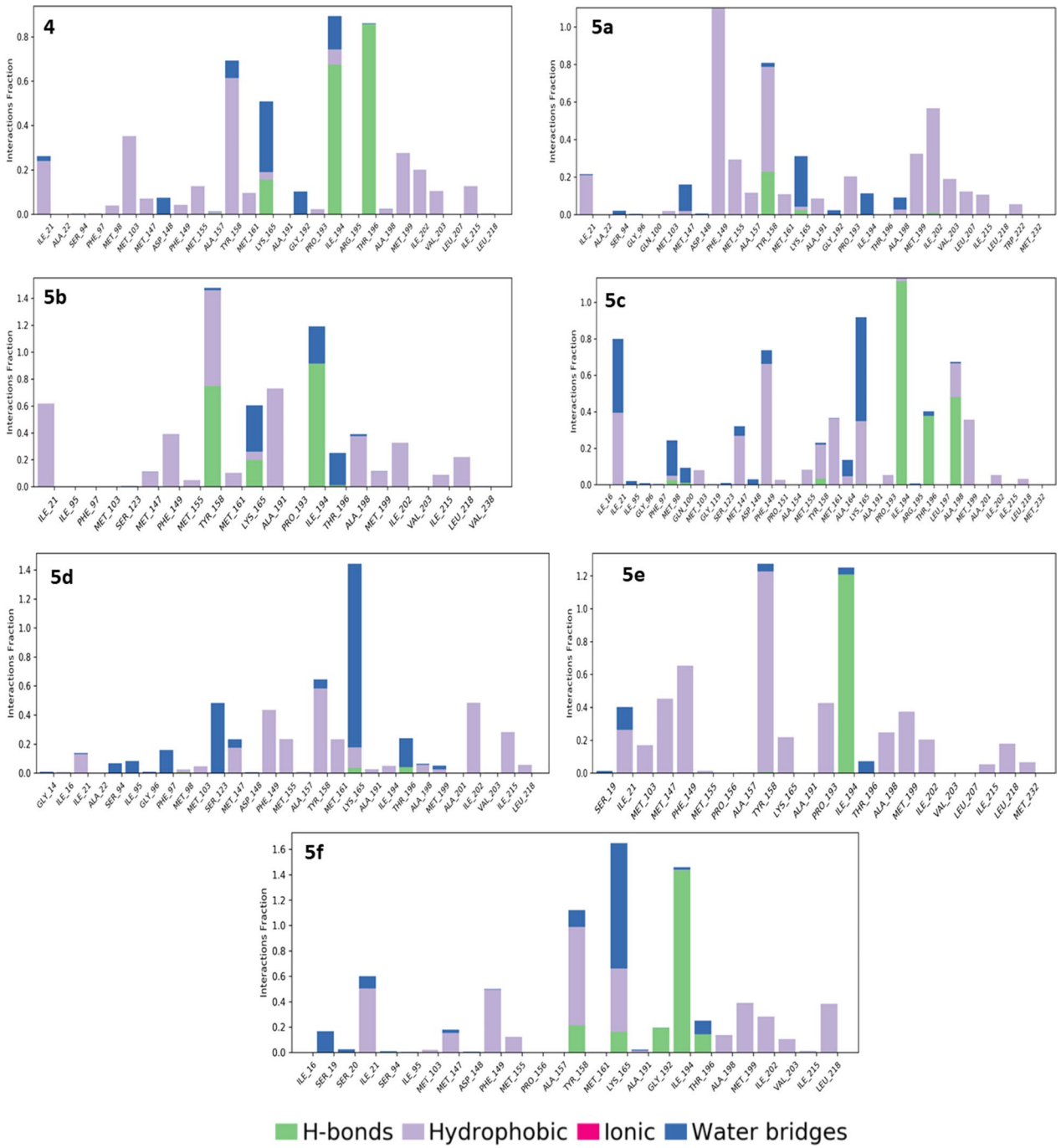

Fig. 4 Ligand–protein contact histogram of lead compounds. The green bar indicates H-bond interaction, the blue bar indicates water-mediated H-bond interaction and the violet bar indicates hydrophobic interaction between the ligand and the protein

may have excellent oral absorption. Furthermore, values established from the parameter, % Human oral absorption, emphasize a very good oral absorption of the novel compounds which also corresponds to better oral bioavailability. As per the MM\GBSA ΔG_{bind} prediction by PRIME, the above seven hits obtained from the docking study showed that test compounds have a good binding affinity toward the receptors. More negative the value, the better the binding affinity.

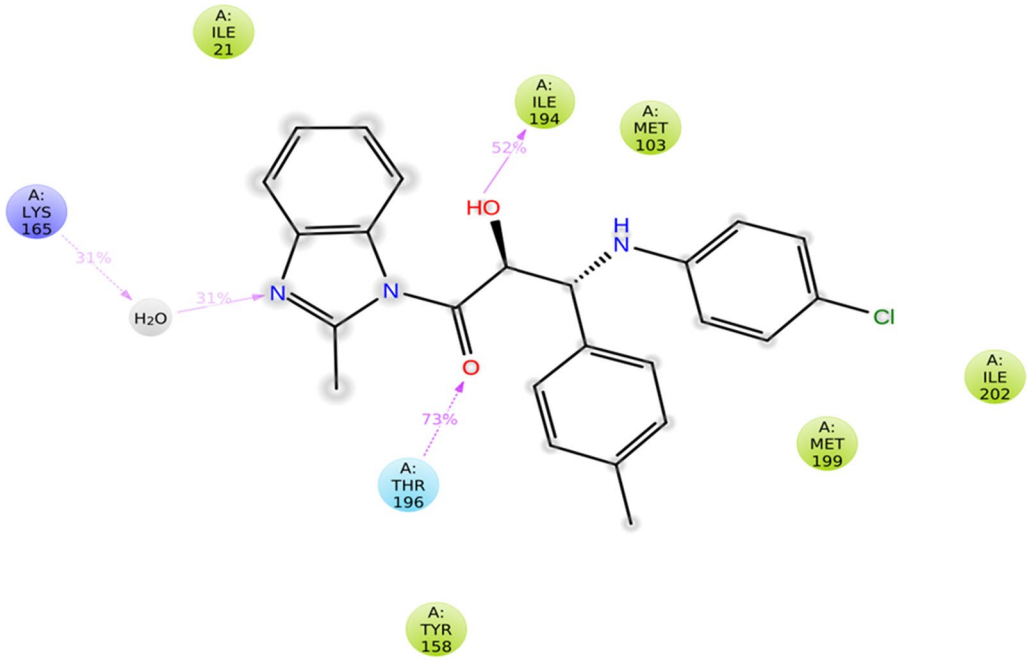

Compound 4

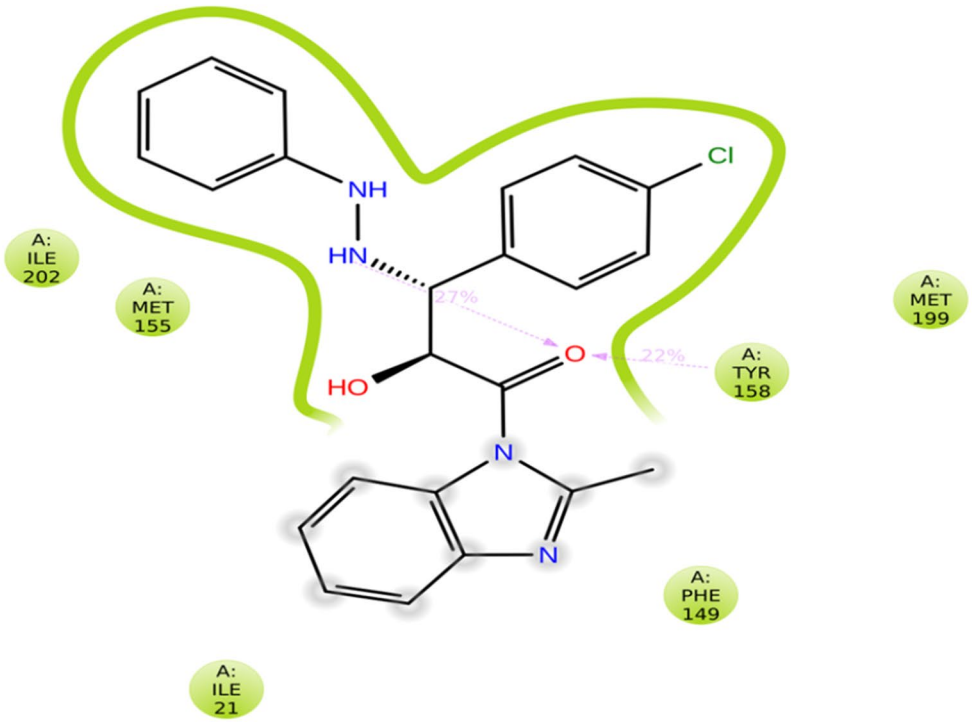

Compound 5a

Fig. 5 Ligand–protein contact of lead compounds. A diagram of the detailed interactions between the ligand atoms and the protein residues. In the chosen trajectory (0.00–50.05 nsec), interactions that occur more than 20.0% of the simulation period are displayed. As some residues may have many contacts of a single kind with the same ligand atom, it is feasible to have interactions with > 100%

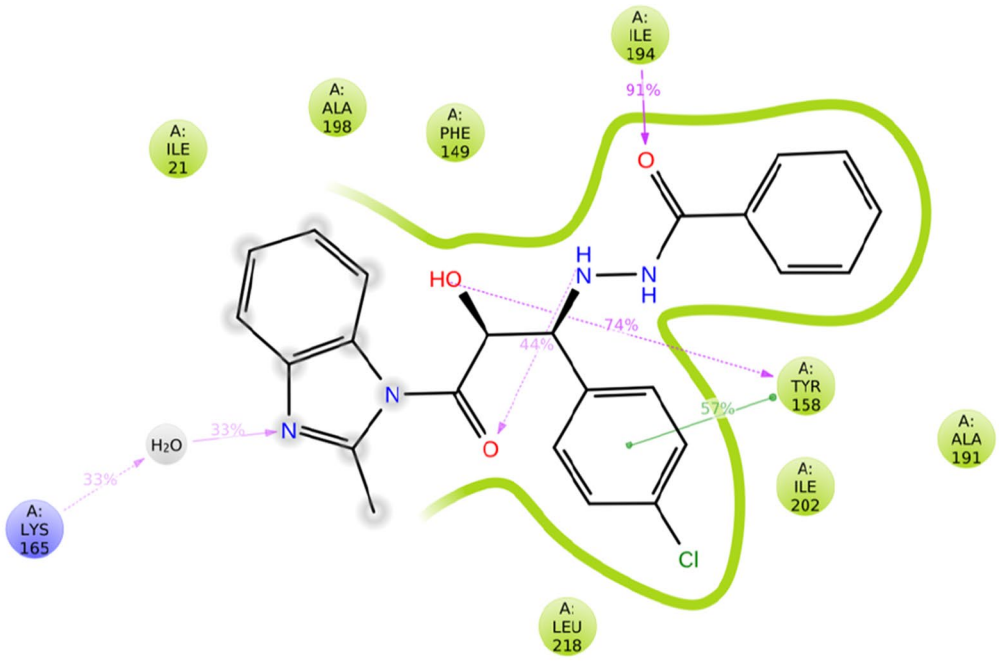

Compound 5b

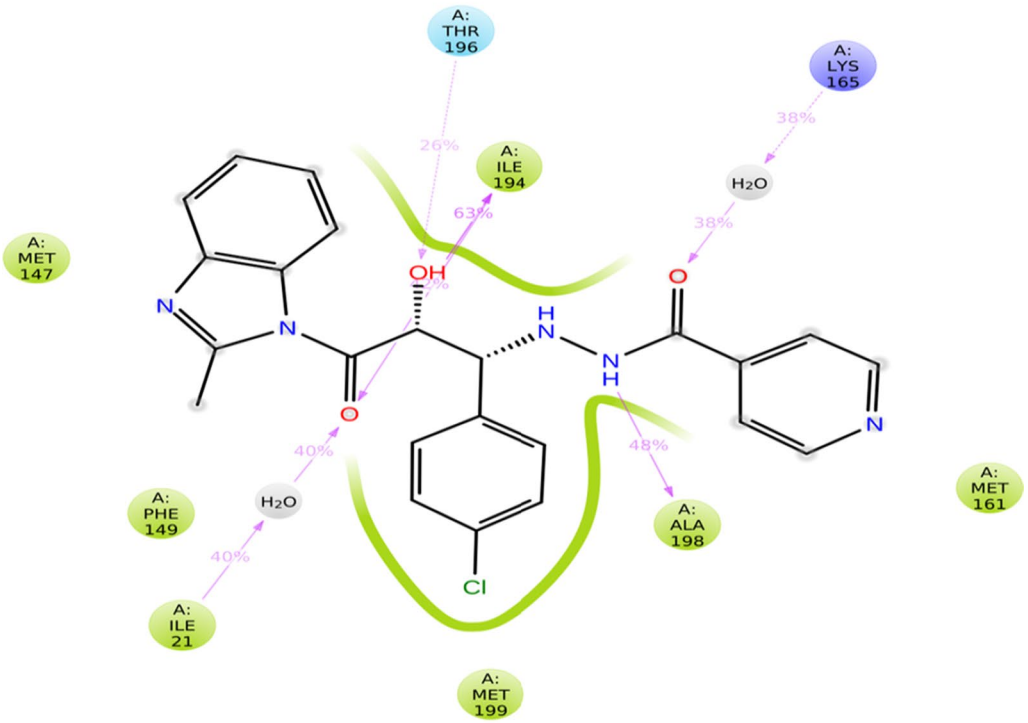

Compound 5c

Fig. 5 continued

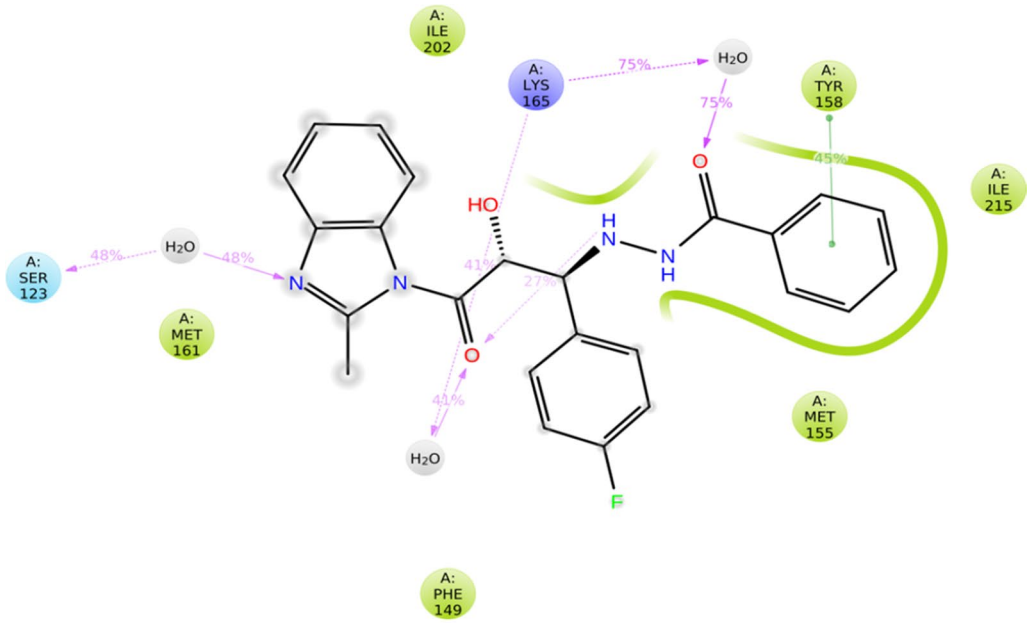

Compound 5d

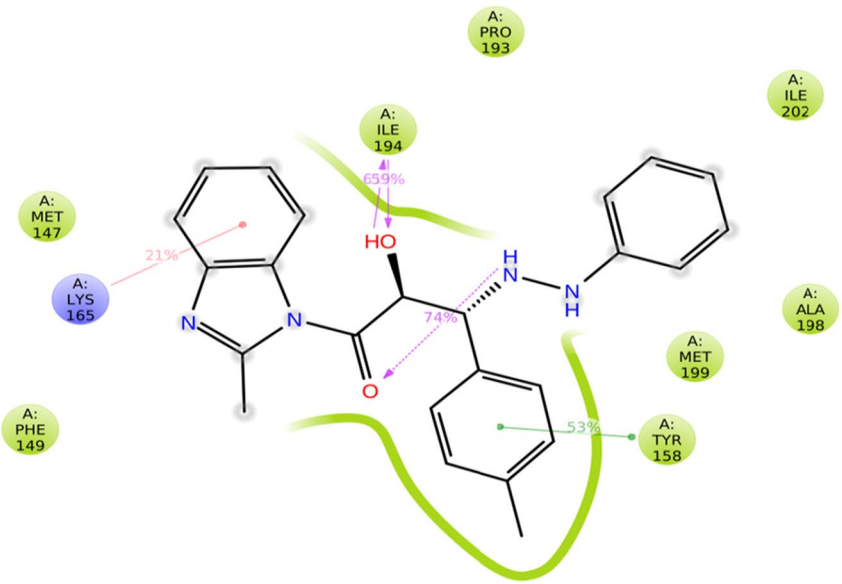

Compound 5e

Fig. 5 continued

Further, an observation made by docking study showed TYR 158, ILE 194 and PHE 149 were critical during the InhA inhibition. Interestingly, all the seven compounds which were chosen for the synthesis demonstrated a similar kind of interaction along with standard INH. Also, the greater number of favorable interaction (TYR 158, ILE 194 and PHE 149) was observed in case of compound 5c, 5a, and 4. This observation improved the level of confidence during the study, and we proceeded with the synthesis of seven novel molecules.

In-vitro biological screening was carried out for the seven synthesized novel benzimidazolyl hydrazide and amino derivatives. The compounds 5d & 5f possess an

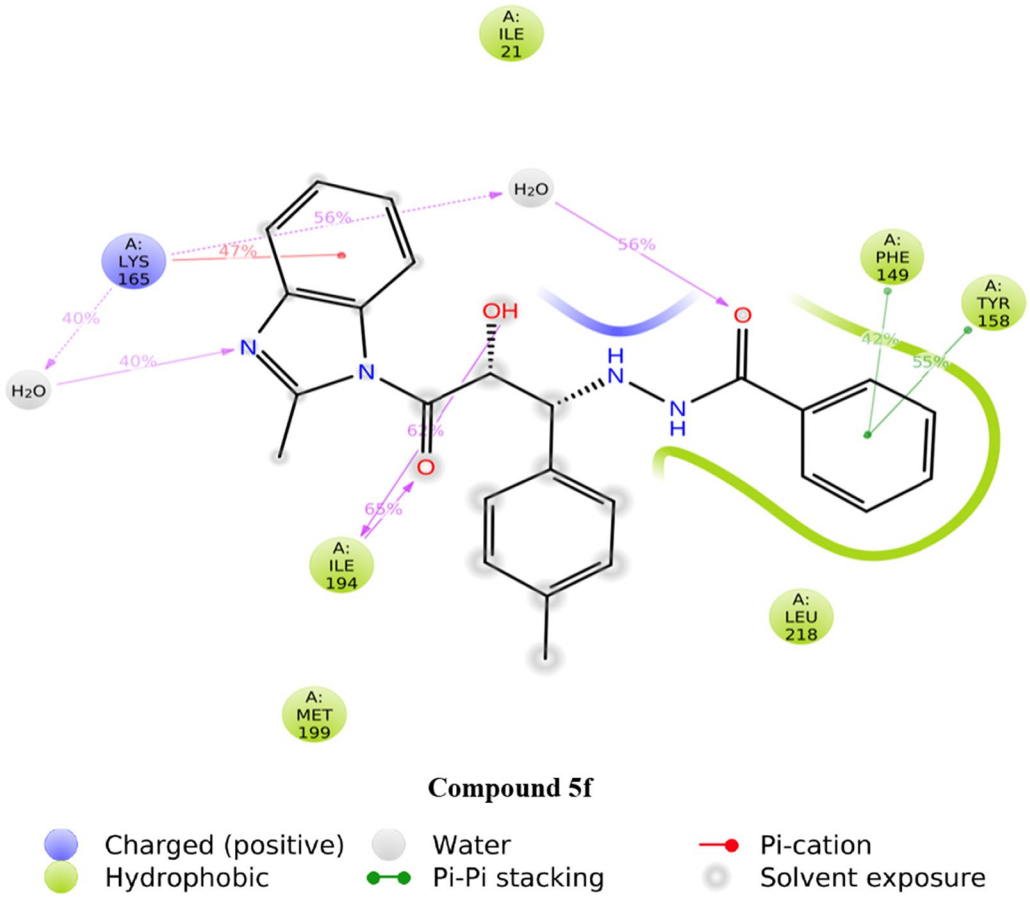

Fig. 5 continued

inhibitory concentration of 5 µg/ml, Compound 5b & 5e have 1 µg/ml, and 4, 5a, and 5c exhibit an inhibitory concentration of 0.5 µg/ml as per the Alamar blue technique which is equivalent to that of the marketed standard drug INH. Interestingly, the *in-vitro* study was strongly correlated with the in-silico prediction, where by compound 4, 5a, and 5c showed greater number of favorable interactions. The chlorophenyl group seems to be an essential chemical segment in the novel molecule which contributes to the property of drug likeliness. The result from the *in-vitro* assay significantly correlated with the binding free energy prediction. This shows how crucial is drug designing in the process of drug discovery.

On account of the remarkable properties of Benzimidazoles, a series of derivatives with modifications have been virtually screened and synthesized to optimize their potency. By carrying out an *in-vitro* study (Alamar Blue assay), all the synthesized novel molecules were screened for antimycobacterial potentials against the strain, *Mycobacterium tuberculosis* H37 Rv strain using the standard INH. The compounds 4, 5a, and 5c displayed the most potent inhibitory activity possessing a MIC of 0.5 µg/ml which is equivalent to the standard drug INH. The presence of a carboxylic linker (–COOH–) between benzimidazole and the rest of the structure of the lead compounds was found to be crucial for activity as the oxygen atom and hydroxyl group of the linker formed most of the favorable interactions. The presence of the chlorophenyl group attached to the 3-oxo-propyl moiety in compound 4, 5a, and 5c dramatically enhances the antimycobacterial activity which is in line with the previous findings [6, 14]. This might be due to hydrophobic interaction with PHE 149 as presence of Cl in the para position of benzyl moiety is in close proximity of hydrophobic pocket in the target binding site [6]. When the chlorophenyl group in compounds 5e and 5f is replaced with a tolyl group, the MIC value changes to 1 g/ml and 5 g/ml, respectively. A similar pattern was also observed where replacing chlorine atom with methyl and cyano group in the para position of benzimidazole completely abolished the

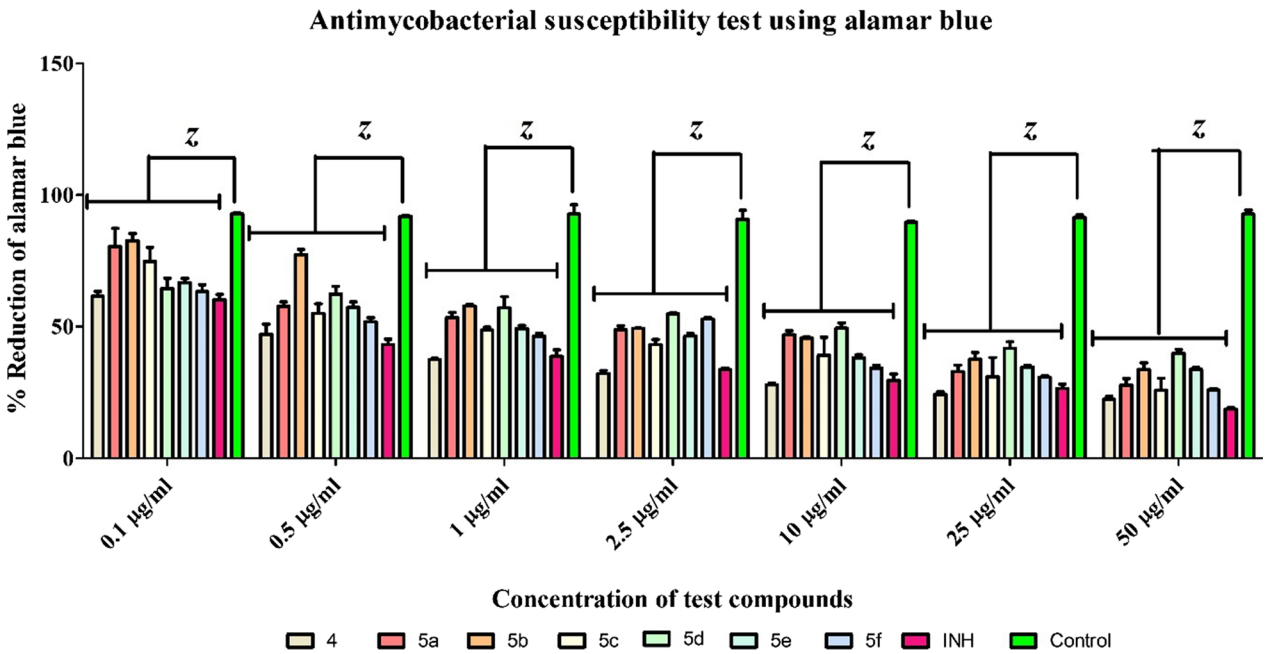

Fig. 6 Antimicrobial susceptibility test. The percentage reduction of Alamar blue (resazurin) to resorufin is a direct indication of mycobacterial viability. A lower percentage reduction of Alamar blue indicates greater mycobacterial susceptibility. The experiment was performed in a 96-well plate in duplicate. The data are expressed as Mean ± SD. The effective dose (LD50) of the compound 4, 5a, 5b, 5c, 5d, 5e, 5f and INH are 0.52, 0.56, 1.02, 0.57, 5.38, 0.95, 5.13, and 0.51 µg/ml respectively at which 50% of the mycobacterial cell death was observed. In case of control (saline), approximately > 90% of mycobacterial cells were viable. When compared to the control there was a significant percentage reduction of Alamar blue in all the groups, whereas when compared to INH there was no significant difference found. The superscript ^{Z} denotes statistical significance at $p < 0.001$. All statistical data were calculated using GraphPad Prism 5

antimycobacterial activity [40]. Furthermore, 3-phenylamino, 3-phenylhydrazino, or 3-iso-nicotinyl hydrazino attachment to the third carbon atom of the oxo-propyl group had no significant effect on the antimycobacterial activity. Additionally, the presence of nitrogen in the amino, hydrazino, or iso-nicotinyl hydrazino group appears to be crucial for the activity. Thus, the addition of a substituted tolyl anilino group to 2-methyl benzimidazole has a significant impact on the product's ability to function as a lead compound. The use of benzimidazole instead of the isonicotinic acid hydrazide group helped to produce promising in-vitro antimycobacterial activity.

Conclusion

The present approach was made, having in mind the life-threatening nature of Tuberculosis as one of the thrust areas of drug research. The integrated analysis from the in-silico prediction and the wet lab experimentation may provide insights into designing novel antimycobacterial agents from a series of 2-substituted benzimidazolyl derivatives. This also proves that computer-aided molecular design techniques are fruitful in rational drug design. This could be a constructive attempt aimed to develop the next generation antitubercular InhA inhibitors for the treatment of multiple drug-resistant tuberculosis.

Limitation and future prospectives

The R and S configuration of the lead compounds was not included in the current study. Our future study plan will include R and S configuration as well as group projection priority.

Abbreviations

TB: Tuberculosis; Mtb: *Mycobacterium tuberculosis*; INH: Isoniazid; FAS II: Fatty acid synthetase II; InhA: Enoyl acyl carrier protein reductase; Kat G: Catalase-peroxidase; TIP3P: Three-site transferable intermolecular potential; ΔG_{bind}: Binding free energy; RMSD: Root mean square deviation; DMF: Dimethylformamide; TLC: Thin-layer chromatography.

Supplementary Information

The online version contains supplementary material available at https://doi.org/10.1186/s43094-022-00449-x.

Additional file 1. Spectral data of lead compounds.

Acknowledgements

We would like to thank Mr. Ranadip Dutta, Department of English, Arunachal University of Studies, Namsai, for syntax and grammar correction.

Author contributions
RKR and AK performed the computational simulations and RKR analyzed the data. UK has conducted all the chemistry and biology-related experiments and UK, RKR and MR have analyzed the data. RKR and UK prepared the manuscript, and RM has revised the manuscript. All authors have read and approved the final manuscript.

Funding
Not applicable.

Availability of data and materials
The data generated or analyzed during this study are included in this published article (and its Additional files).

Declarations

Ethics approval and consent to participate
Not applicable.

Consent of publication
Not applicable.

Competing interest
The authors have no competing interest.

Author details
[1]Department of Pharmaceutical Chemistry, PSG College of Pharmacy, The Tamil Nadu Dr. M.G.R. Medical University, Chennai, India. [2]Department of Pharmacology, PSG College of Pharmacy, The Tamil Nadu Dr. M.G.R. Medical University, Chennai, India. [3]Present Address: Department of Pharmacology, Girijananda Chowdhury Institute of Pharmaceutical Science, Tezpur, India.

Received: 15 July 2022 Accepted: 12 December 2022
Published online: 22 December 2022

References

1. Allard B, Panariti A, Martin JG (2018) Alveolar macrophages in the resolution of inflammation, tissue repair, and tolerance to infection. Front Immunol 9:1777. https://doi.org/10.3389/fimmu.2018.01777
2. Vilchèze C, Wang F, Arai M, Hazbón MH, Colangeli R, Kremer L, Weisbrod TR, Alland D, Sacchettini JC, Jacobs WR (2006) Transfer of a point mutation in Mycobacterium tuberculosis inhA resolves the target of isoniazid. Nat Med 12:1027–1029. https://doi.org/10.1038/nm1466
3. Lu XY, You QD, Chen YD (2010) Recent progress in the identification and development of InhA direct inhibitors of *Mycobacterium tuberculosis*. MRMC 10:182–193. https://doi.org/10.2174/138955710791185064
4. Sivakumaran D, Jenum S, Vaz M, Selvam S, Ottenhoff THM, Haks MC, Malherbe ST, Doherty TM, Ritz C, Grewal HMS (2020) Combining host-derived biomarkers with patient characteristics improves signature performance in predicting tuberculosis treatment outcomes. Commun Biol 3:359. https://doi.org/10.1038/s42003-020-1087-x
5. Antoci V, Cucu D, Zbancioc G, Moldoveanu C, Mangalagiu V, Amariucai-Mantu D, Aricu A, Mangalagiu II (2020) *Bis*-(imidazole/benzimidazole)-pyridine derivatives: synthesis, structure and antimycobacterial activity. Future Med Chem 12:207–222. https://doi.org/10.4155/fmc-2019-0063
6. Pieroni M, Tipparaju SK, Lun S, Song Y, Sturm AW, Bishai WR, Kozikowski AP (2011) Pyrido[1,2-*a*]benzimidazole-based agents active against tuberculosis (TB), multidrug-resistant (MDR) TB and extensively drug-resistant (XDR) TB. ChemMedChem 6:334–342. https://doi.org/10.1002/cmdc.201000490
7. Rückle T, Biamonte M, Grippi-Vallotton T, Arkinstall S, Cambet Y, Camps M, Chabert C, Church DJ, Halazy S, Jiang X, Martinou I, Nichols A, Sauer W, Gotteland J-P (2004) Design, synthesis, and biological activity of novel, potent, and selective (benzoylaminomethyl)thiophene sulfonamide inhibitors of c-Jun-N-terminal kinase. J Med Chem 47:6921–6934. https://doi.org/10.1021/jm031112e
8. Ang CW, Tan L, Sykes ML, AbuGharbiyeh N, Debnath A, Reid JC, West NP, Avery VM, Cooper MA, Blaskovich MAT (2020) Antitubercular and antiparasitic 2-nitroimidazopyrazinones with improved potency and solubility. J Med Chem 63:15726–15751. https://doi.org/10.1021/acs.jmedchem.0c01372
9. Cheng Y-J, Liu Z-Y, Liang H-J, Fang C-T, Zhang N-N, Zhang T-Y, Yan M (2019) Discovery of (3-Benzyl-5-hydroxyphenyl)carbamates as new antitubercular agents with potent in vitro and in vivo efficacy. Molecules 24:2021. https://doi.org/10.3390/molecules24102021
10. Karczmarzyk Z, Swatko-Ossor M, Wysocki W, Drozd M, Ginalska G, Pachuta-Stec A, Pitucha M (2020) New application of 1,2,4-triazole derivatives as antitubercular agents. Structure, in vitro screening and docking studies. Molecules 25:6033. https://doi.org/10.3390/molecules25246033
11. Krause M, Foks H, Ziembicka D, Augustynowicz-Kopeć E, Głogowska A, Korona-Głowniak I, Bojanowski K, Siluk D, Gobis K (2020) 4-Substituted picolinohydrazonamides as a new class of potential antitubercular agents. Eur J Med Chem 190:112106. https://doi.org/10.1016/j.ejmech.2020.112106
12. Kasetti AB, Singhvi I, Nagasuri R, Bhandare RR, Shaik AB (2021) Thiazole-chalcone hybrids as prospective antitubercular and antiproliferative agents: design, synthesis, biological, molecular docking studies and in silico ADME evaluation. Molecules 26:2847. https://doi.org/10.3390/molecules26102847
13. Oh S, Libardo MDJ, Azeeza S, Pauly GT, Roma JSO, Sajid A, Tateishi Y, Duncombe C, Goodwin M, Ioerger TR, Wyatt PG, Ray PC, Gray DW, Boshoff HIM, Barry CE (2021) Structure-Activity Relationships of Pyrazolo[1,5-a]pyrimidin-7(4 *H*)-ones as Antitubercular Agents. ACS Infect Dis 7:479–492. https://doi.org/10.1021/acsinfecdis.0c00851
14. Jiménez-Juárez R, Cruz-Chávez W, de Jesús-Ramírez N, Castro-Ramírez GI, Uribe-González I, Martínez-Mejía G, Ruiz-Nicolás R, Aguirre-Alvarado C, Castrejón-Jiménez NS, García-Pérez BE (2020) Synthesis and antimycobacterial activity of 2,5-disubstituted and 1,2,5-trisubstituted benzimidazoles. Front Chem 8:433. https://doi.org/10.3389/fchem.2020.00433
15. Cade CE, Dlouhy AC, Medzihradszky KF, Salas-Castillo SP, Ghiladi RA (2010) Isoniazid-resistance conferring mutations in *Mycobacterium tuberculosis* KatG: Catalase, peroxidase, and INH-NADH adduct formation activities: Isoniazid-Resistance Conferring Mutations in *Mtb* KatG. Protein Sci 19:458–474. https://doi.org/10.1002/pro.324
16. Hsu L-Y, Lai L-Y, Hsieh P-F, Lin T-L, Lin W-H, Tasi H-Y, Lee W-T, Jou R, Wang J-T (2020) Two novel *katG* Mutations Conferring Isoniazid Resistance in *Mycobacterium tuberculosis*. Front Microbiol 11:1644. https://doi.org/10.3389/fmicb.2020.01644
17. Dar AM, Mir S (2017) Molecular docking: approaches, types, applications and basic challenges. J Anal Bioanal Tech. https://doi.org/10.4172/2155-9872.1000356
18. A.I. (Arthur I. Vogel, Vogel's textbook of quantitative chemical analysis, Fifth edition / [revised by ... G.H. Jeffery ... [and others]. Harlow, Essex, England : Longman Scientific & Technical ; New York : Wiley, 1989. https://search.library.wisc.edu/catalog/999612906602121.
19. Finar IL (1975) Organic chemistry. 2: Stereochemistry and the chemistry of natural products, 5th edn. Longmans, London
20. Sykes P (1970) A guidebook to mechanism in organic chemistry, 3rd edn. Longmans, Harlow
21. Morrison RT, Boyd RN (1992) Organic chemistry, 6th edn. Prentice Hall, Englewood, Cliffs, N.J.
22. Vijayakumar S, Manogar P, Prabhu S, Sanjeevkumar Singh RA (2018) Novel ligand-based docking; molecular dynamic simulations; and absorption, distribution, metabolism, and excretion approach to analyzing potential acetylcholinesterase inhibitors for Alzheimer's disease. J Pharm Anal 8:413–420. https://doi.org/10.1016/j.jpha.2017.07.006
23. Collins L, Franzblau SG (1997) Microplate alamar blue assay versus BACTEC 460 system for high-throughput screening of compounds against *Mycobacterium tuberculosis* and Mycobacterium avium. Antimicrob Agents Chemother 41:1004–1009
24. Roy S, Sharma S, Sharma M, Aggarwal R, Bose M (2004) Induction of nitric oxide release from the human alveolar epithelial cell line A549: an in vitro correlate of innate immune response to *Mycobacterium tuberculosis*. Immunology 112:471–480. https://doi.org/10.1046/j.1365-2567.2004.01905.x
25. Collee JG (1996) Practical medical microbiology, Churchill Livingstone. Edinburgh, New York
26. Cappuccino JG, Sherman N (1992) Microbiology: a laboratory manual, 3rd edn. Benjamin/Cummings Pub. Co, Redwood City, Calif

27. Vogel AI, Bassett J (1978) Vogel's textbook of quantitative inorganic analysis: including elementary instrumental analysis, 4th edn. Longman, London, New York
28. Krishnan VSH, Chowdary KS, Dubey PK, Vijaya S (2010) ChemInform Abstract: Studies on the Synthesis of 2-Phenylsulfonyl-3-styrylquinoxalines. ChemInform. https://doi.org/10.1002/chin.200140147
29. Pan P, Tonge PJ (2012) Targeting InhA, the FASII Enoyl-ACP reductase: SAR studies on novel inhibitor scaffolds. CTMC 12:672–693. https://doi.org/10.2174/156802612799984535
30. He X, Alian A, Ortiz de Montellano PR (2007) Inhibition of the *Mycobacterium tuberculosis* enoyl acyl carrier protein reductase InhA by arylamides. Bioorganic Med Chem 15:6649–6658. https://doi.org/10.1016/j.bmc.2007.08.013
31. Xia Y, Zhou Y, Carter DS, McNeil MB, Choi W, Halladay J, Berry PW, Mao W, Hernandez V, O'Malley T, Korkegian A, Sunde B, Flint L, Woolhiser LK, Scherman MS, Gruppo V, Hastings C, Robertson GT, Ioerger TR, Sacchettini J, Tonge PJ, Lenaerts AJ, Parish T, Alley M (2018) Discovery of a cofactor-independent inhibitor of *Mycobacterium tuberculosis* InhA. Life Sci. Alliance 1:e201800025. https://doi.org/10.26508/lsa.201800025
32. Desai N, Bhavsar A, Baldaniya B (2009) Synthesis and antimicrobial activity of 5-imidazolinone derivatives. Indian J Pharm Sci 71:90. https://doi.org/10.4103/0250-474X.51953
33. Ahluwalia VK, Tyagi R, Khurana A (2010) ChemInform Abstract: synthesis of 3-(Thiadiazol-2-ylthio-, Pyridin-2-ylthio- and Benzimidazol-2-ylthio)-2H-1-benzopyran-2-ones. ChemInform. https://doi.org/10.1002/chin.199122145
34. Chauhan PM, Sunduru N, Sharma M (2010) Recent advances in the design and synthesis of heterocycles as anti-tubercular agents. Future Med Chem 2:1469–1500. https://doi.org/10.4155/fmc.10.227
35. Nguyen Tien C, Tran Thi Cam D, Bui Manh H, Nguyen Dang D (2016) Synthesis and antibacterial activity of some derivatives of 2-methylbenzimidazole containing 1,3,4-oxadiazole or 1,2,4-triazole heterocycle. J Chem. https://doi.org/10.1155/2016/1507049
36. Hameed P S, Raichurkar A, Madhavapeddi P, Menasinakai S, Sharma S, Kaur P, Nandishaiah R, Panduga V, Reddy J, Sambandamurthy VK, Sriram D (2014) Benzimidazoles: novel mycobacterial gyrase inhibitors from scaffold morphing. ACS Med Chem Lett 5:820–825. https://doi.org/10.1021/ml5001728
37. Kumar K, Awasthi D, Lee S-Y, Zanardi I, Ruzsicska B, Knudson S, Tonge PJ, Slayden RA, Ojima I (2011) Novel trisubstituted benzimidazoles, targeting *Mtb* FtsZ, as a new class of antitubercular agents. J Med Chem 54:374–381. https://doi.org/10.1021/jm1012006
38. Marrakchi H, Lanéelle G, Quémard A (2000) InhA, a target of the antituberculous drug isoniazid, is involved in a mycobacterial fatty acid elongation system, FAS-II. Microbiology 146:289–296. https://doi.org/10.1099/00221287-146-2-289
39. Mehboob S, Hevener KE, Truong K, Boci T, Santarsiero BD, Johnson ME (2012) Structural and enzymatic analyses reveal the binding mode of a novel series of *Francisella tularensis* Enoyl Reductase (FabI) inhibitors. J Med Chem 55:5933–5941. https://doi.org/10.1021/jm300489v
40. Venugopala KN, Chandrashekharappa S, Deb PK, Tratrat C, Pillay M, Chopra D, Al-Shar'i NA, Hourani W, Dahabiyeh LA, Borah P, Nagdeve RD, Nayak SK, Padmashali B, Morsy MA, Aldhubiab BE, Attimarad M, Nair AB, Sreeharsha N, Haroun M, Shashikanth S, Mohanlall V, Mailavaram R (2021) Anti-tubercular activity and molecular docking studies of indolizine derivatives targeting mycobacterial InhA enzyme. J Enzyme Inhib Med Chem 36:1471–1486. https://doi.org/10.1080/14756366.2021.1919889

Publisher's Note